Chalcogenide Letters Vol. 21, No. 10, October 2024, p. 785 - 796

Development of SBS composite modified asphalt incorporating polydopamine-enhanced MoS_2

Y. L. Hou*, L. Z Bai
Department of Railway Engineering, Zhengzhou Railway Vocational and Technical College, Zhengzhou 451460, China

This study investigated the development of a novel composite modified asphalt incorporating PDA-MoS_2 into styrene-butadiene-styrene (SBS) modified asphalt. The successful synthesis of PDA-MoS_2 was confirmed through various characterization techniques. The incorporation of PDA-MoS_2 into SBS modified asphalt resulted in significant improvements in performance properties. With a PDA-MoS_2 content of 0.7 wt%, the modified asphalt showed a notable 15.1% rise in softening point and a 24% drop in penetration in comparison to the control SBS modified asphalt. Dynamic Shear Rheometer tests revealed a 2.4-fold increase in the rutting factor at 60°C. Multiple Stress Creep Recovery tests demonstrated enhanced rutting resistance, with a 72.2% reduction in non-recoverable creep compliance at 0.1 kPa stress level. Electrochemical measurements showed improved corrosion resistance, evidenced by lower current densities and higher charge transfer resistance. Microstructural analysis revealed well-dispersed PDA-MoS_2 particles forming a compact network structure within the asphalt matrix. The hydrophilicity of the modified asphalt increased, with a 35.3% decrease in water contact angle. The synergistic effect between PDA-MoS2, SBS, and asphalt components, facilitated by enhanced interfacial interactions and chemical bonding, contributed to the observed performance improvements. The results indicate that PDA-MoS_2 has the potential to improve the characteristics of SBS modified asphalt as a modifier.

(Received June 27, 2024; Accepted October 7, 2024)

Keywords: Rheological properties, Rutting resistance, Hydrophilicity, Corrosion resistance, Microstructure

1. Introduction

Asphalt is a widely used material in the construction and maintenance of road infrastructure. However, the performance of conventional asphalt often falls short in meeting the increasing demands of modern transportation, especially under heavy traffic loads and extreme weather conditions [1,2]. In order to tackle these obstacles, scientists have investigated different approaches to alter asphalt and improve its characteristics. One potential method involves integrating polymers, like SBS, into the composition of the asphalt mixture [3]. SBS polymer modified asphalt has shown

* Corresponding author: 17319777020@163.com
https://doi.org/10.15251/CL.2024.2110.785

improved flexibility, crack resistance, and temperature sensitivity compared to unmodified asphalt [4,5]. Despite the benefits of SBS modification, there are still limitations that need to be addressed. The compatibility between SBS and asphalt can be a concern, as phase separation may occur over time, leading to performance degradation [6,7]. Moreover, the high cost of SBS and its potential to undergo oxidative degradation during high-temperature mixing and aging can hinder its widespread application [8]. Hence, it is essential to investigate different additives that can improve the characteristics of SBS modified asphalt and address these challenges.

Recently, molybdenum disulfide (MoS_2) has attracted attention as a potential asphalt modifier due to its unique layered structure and excellent mechanical properties [9,10]. MoS_2 possesses high strength, good flexibility, and remarkable lubricating properties, which can contribute to improved rutting resistance and fatigue performance of asphalt [11]. Additionally, the two-dimensional structure of MoS_2 allows for easy dispersion in the asphalt matrix, promoting homogeneity and stability of the modified asphalt. However, the hydrophobic nature of MoS_2 can pose challenges in its application as an asphalt modifier. The poor water wettability of MoS_2 can hinder its interaction with the asphalt binder, leading to inadequate dispersion and weak interfacial bonding [12,13]. This may lead to decreased efficiency and longevity of the altered asphalt. Hence, there is a need to discover methods to boost the hydrophilicity of MoS_2 and enhance its harmonization with the asphalt mixture.

Polydopamine (PDA) has emerged as a promising solution to address the hydrophilicity issues of MoS_2 [14,15]. It possesses excellent adhesive properties and can form stable coatings on various surfaces through self-polymerization. By modifying MoS_2 with PDA, it is possible to improve its water wettability and enhance its interaction with the asphalt binder [16]. The hydrophilic nature of PDA can facilitate the dispersion of MoS_2 in the asphalt matrix, leading to improved homogeneity of the asphalt [17,18]. The objectives of this study are twofold. First, we aim to develop a novel composite modified asphalt by incorporating PDA-enhanced MoS_2 into SBS modified asphalt. By combining the benefits of SBS, MoS_2, and PDA, we expect to achieve superior performance compared to conventional SBS modified asphalt. Second, we intend to investigate the mechanisms behind the property enhancement of the composite modified asphalt, focusing on the role of PDA in improving the hydrophilicity and compatibility of MoS_2 with the asphalt matrix. The novelty of this study lies in the synergistic utilization of PDA, MoS_2, and SBS to create a high-performance composite asphalt. By leveraging the unique properties of each component and the synergistic effects between them, we aim to develop an innovative asphalt material with enhanced mechanical, rheological, and durability characteristics.

2. Materials and methods

2.1. Materials

The base asphalt binder used in this study was SK-70A, obtained from SK Energy Co., Ltd. (Ulsan, South Korea). The asphalt had a penetration grade of 60/70 and met the specifications requirements of China. The SBS polymer (YH-791) was supplied by Sinopec Baling Company (Yueyang, China) with a styrene content of 30% and a block ratio of 30/70. Molybdenum disulfide (MoS_2) was purchased from Alfa Aesar (Shanghai, China). Dopamine hydrochloride (98%), tris(hydroxymethyl)aminomethane (Tris) was obtained from Sinopharm Chemical Reagent Co., Ltd. (Shanghai, China).

2.2. Synthesis of polydopamine-modified MoS_2 (PDA-MoS_2)

The production of PDA-MoS_2 was achieved using a self-polymerization technique. To start, 1 g of MoS_2 powder was mixed with 100 milliliters of Tris-HCl buffer solution (10 mM, pH 8.5) using ultrasonication for 30 minutes until a consistent suspension was formed. Next, the suspension was supplemented with 1 g of dopamine hydrochloride, followed by stirring at room temperature for a duration of 24 hours. During this process, the self-polymerization of dopamine occurred, forming a PDA coating on the surface of MoS_2. Following the reaction, the PDA-MoS_2 particles were harvested through centrifugation at 8000 rpm for 10 minutes, rinsed with water, and then dehydrated in a vacuum oven at 60°C for 12 hours.

2.3. Development of SBS composite modified asphalt with the addition of PDA-MoS_2

The preparation of SBS composite modified asphalt incorporating PDA-MoS_2 involved a melt blending process. Initially, the base asphalt was heated to 170°C in a temperature-controlled oil bath. Then, 5 wt% of SBS polymer was gradually added to the asphalt under high-speed shearing at 5000 rpm for 1 h. After the SBS was completely dissolved and the mixture became homogeneous, a designated amount of PDA-MoS_2 (0.1, 0.3, 0.5, and 0.7 wt% by weight of asphalt) was introduced into the SBS modified asphalt. The blending continued for another 1 h at 5000 rpm to ensure uniform dispersion of PDA-MoS_2 in the asphalt matrix. The resulting composite modified asphalt samples were labeled as PDA-MoS_2/SBS, with the number indicating the weight percentage of PDA-MoS_2.

3. Results and discussion

3.1. Characterization of PDA-MoS2

The morphology and microstructure of MoS_2 before and after PDA modification were investigated using SEM. As shown in Figure 1a, the pristine MoS_2 particles exhibited a typical layered structure with smooth surfaces and sharp edges. The particles were relatively uniform in size, ranging from 1 to 3 μm. After the self-polymerization of dopamine, the PDA-MoS_2 particles (Figure 1b) displayed a rougher surface morphology compared to pristine MoS_2. The PDA coating formed a thin and homogeneous layer on the surface of MoS_2 particles, which slightly increased their size. The PDA coating also led to the formation of some interconnected structures between the MoS_2 particles, indicating improved interactions and potential for better dispersion in the asphalt matrix.

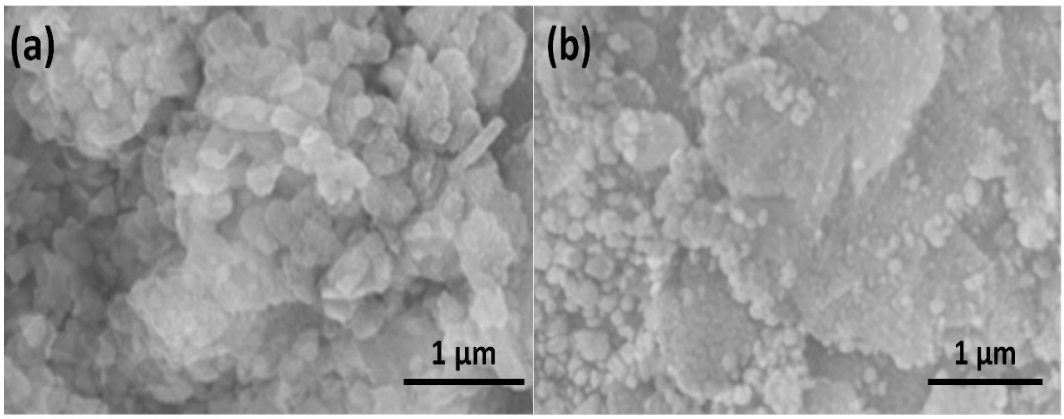

Fig. 1. SEM images of (a) pristine MoS_2 and (b) PDA-MoS_2.

The XRD patterns of MoS_2 and PDA-MoS_2 are presented in Figure 2. The pure MoS2 exhibited distinct diffraction peaks at angles of 14.3°, 32.8°, 39.4°, and 58.2°, which can be attributed to the (002), (100), (103), and (110) planes of the hexagonal MoS_2 structure (JCPDS No.

37-1492) [19], respectively. After PDA modification, the PDA-MoS_2 sample exhibited similar diffraction peaks, suggesting that the crystal structure of MoS_2 was maintained. However, a slight decrease in peak intensity was observed for PDA-MoS_2, which could be attributed to the presence of the amorphous PDA coating [20]. The XRD results confirmed that the PDA modification did not alter the inherent crystal structure of MoS_2.

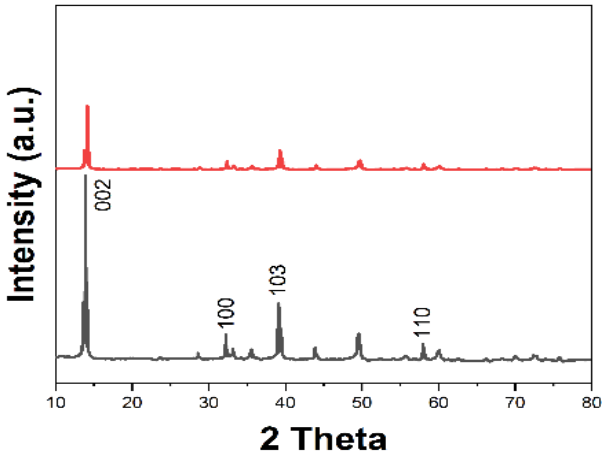

Fig. 2. XRD patterns of MoS_2 and PDA-MoS_2.

The identification of functional groups and chemical bonds in MoS_2 and PDA-MoS_2 was carried out using FTIR spectroscopy. As shown in Figure 3, the pristine MoS_2 exhibited a characteristic peak at 468 cm^{-1}, which corresponded to the Mo-S stretching vibration [21]. Following the modification with PDA, the PDA-MoS_2 sample exhibited new peaks at 1615 cm^{-1} and 1510 cm^{-1}, which were identified as the C=C stretching vibration of aromatic rings within the PDA structure. The broad peak at around 3400 cm^{-1} was attributed to the O-H stretching vibration of catechol hydroxyl groups in PDA [22]. Furthermore, the peaks observed at 1288 cm^{-1} and 1120 cm^{-1} were identified as originating from the stretching vibrations of C-O and C-N in PDA [23], respectively. The FTIR analysis verified that PDA was effectively applied onto the MoS_2 particles by undergoing self-polymerization of dopamine.

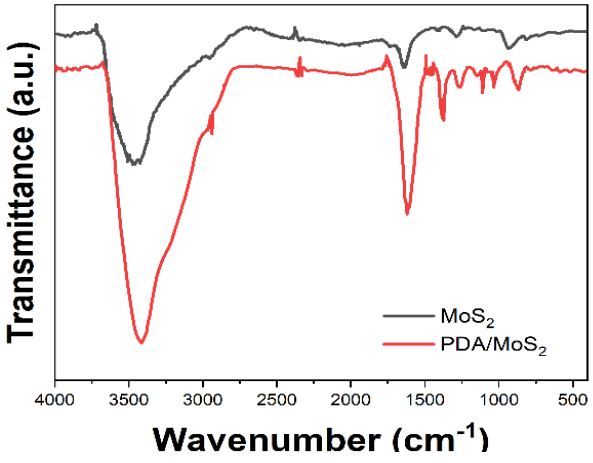

Fig. 3. FTIR spectra of MoS_2 and PDA-MoS_2.

3.2. Evaluation of SBS composite modified asphalt incorporating PDA-MoS_2

The impact of varying levels of PDA-MoS_2 on the traditional performance characteristics of SBS-modified asphalt was examined. The softening point of the SBS modified asphalt increased, while the penetration decreased with the addition of PDA-MoS2, as shown in Table 1. The softening point increased from 68.2°C for the control sample to 78.5°C for the SBS modified asphalt with 0.7 wt% PDA-MoS_2, indicating enhanced temperature stability. The penetration decreased from 52.8 dmm for the control sample to 40.1 dmm for the 0.7 wt% PDA-MoS_2 modified asphalt, suggesting improved stiffness and resistance to deformation [24]. The addition of PDA-MoS_2 resulted in a reduction in the ductility of the modified asphalt. However, even with increasing PDA-MoS_2 content, all samples still exhibited ductility values exceeding 10 cm, meeting the requirements for use in asphalt pavement [25].

Table 1. Distinctive performance characteristics of SBS modified asphalt with varying levels of PDA-MoS_2.

PDA-MoS_2 Content (wt%)	Softening Point (°C)	Penetration (dmm)	Ductility (cm)
0 (Control)	68.2 ± 0.3	52.8 ± 1.2	65.3 ± 2.1
0.1	70.5 ± 0.4	49.3 ± 0.5	58.7 ± 1.2
0.3	73.8 ± 0.3	45.6 ± 0.9	42.1 ± 1.1
0.5	76.2 ± 0.5	42.7 ± 1.1	28.4 ± 1.3
0.7	78.5 ± 0.2	40.1 ± 0.8	18.9 ± 0.8

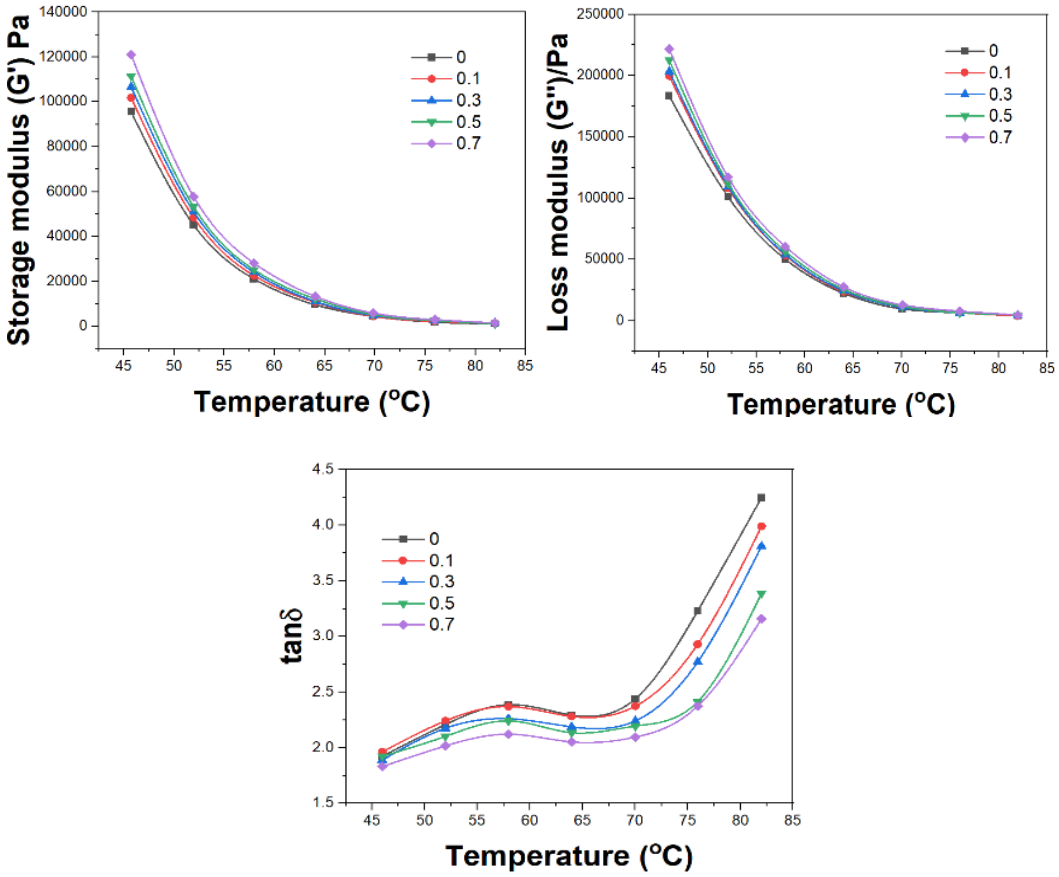

Fig. 4. G', G" and tanδ of SBS-asphalt with different PDA-MoS_2 contents at 60°C.

Table 2. G/sin δ of SBS-asphalt with different PDA-MoS_2 contents at 60°C.*

PDA-MoS_2 Content (wt%)	Rutting Factor (G*/sin δ) at 60°C (kPa)
0 (Control)	1.62 ± 0.08
0.1	2.05 ± 0.11
0.3	2.74 ± 0.07
0.5	3.38 ± 0.12
0.7	3.85 ± 0.14

The viscoelastic properties of the SBS modified asphalt with different PDA-MoS_2 contents were evaluated using DSR. Figure 4 presents the storage modulus (G'), loss modulus (G'') and phase angle (tanδ) of the asphalt samples at 60°C. The incorporation of PDA-MoS_2 significantly increased the G* values and decreased the δ values compared to the control sample. The increased G* indicates improved stiffness and resistance to deformation, while the decreased δ suggests enhanced elastic behavior [26]. The rutting factor increased with increasing PDA-MoS_2 content, as shown in Table 2. The 0.7 wt% PDA-MoS_2-asphalt exhibited the highest rutting factor, which is 2.4 times higher than that of the control sample. The improved viscoelastic properties of the PDA-MoS_2 modified asphalt can be attributed to the reinforcing effect of the well-dispersed PDA-MoS_2 particles and the strong interactions between PDA-MoS_2 and the asphalt matrix.

The MSCR test was used to assess the rutting resistance of the SBS modified asphalt with PDA-MoS_2. Table 3 displays the non-reversible deformation compliance (Jnr) and recovery percentage (R) of the asphalt specimens at a temperature of 60°C. The addition of PDA-MoS_2 significantly reduced the Jnr values and increased the R values compared to the control sample, indicating improved rutting resistance and elastic recovery. The Jnr values decreased from 2.45 kPa^{-1} for the control sample to 0.68 kPa^{-1} for the 0.7 wt% PDA-MoS_2-asphalt at 0.1 kPa stress level, and from 3.21 kPa^{-1} to 0.92 kPa^{-1} at 3.2 kPa stress level. The R values increased from 8.2% for the control sample to 45.6% for the 0.7 wt% PDA-MoS_2 modified asphalt at 0.1 kPa stress level, and from 2.5% to 35.8% at 3.2 kPa stress level. The improved rutting resistance of the PDA-MoS_2 modified asphalt can be attributed to the enhanced stiffness and elasticity provided by the PDA-MoS_2 particles, as well as the strong interfacial bonding between PDA-MoS_2 and the asphalt matrix.

Table 3. Jnr and R of SBS modified asphalt with different PDA-MoS_2 contents at 60°C.

PDA-MoS_2 Content (wt%)	Jnr at 0.1 kPa (kPa^{-1})	Jnr at 3.2 kPa (kPa^{-1})	R at 0.1 kPa (%)	R at 3.2 kPa (%)
0 (Control)	2.45 ± 0.11	3.21 ± 0.07	8.2 ± 0.4	2.5 ± 0.2
0.1	1.98 ± 0.14	2.76 ± 0.11	15.6 ± 0.5	7.8 ± 0.7
0.3	1.42 ± 0.08	2.05 ± 0.08	27.3 ± 0.5	18.5 ± 0.8
0.5	0.95 ± 0.07	1.38 ± 0.02	38.9 ± 0.2	28.7 ± 1.3
0.7	0.68 ± 0.02	0.92 ± 0.05	45.6 ± 0.7	35.8 ± 1.1

The corrosion resistance of the SBS modified asphalt with PDA-MoS_2 was investigated using electrochemical measurements. Figure 5a displays the potentiodynamic polarization curves of the asphalt specimens immersed in a 3.5 wt% NaCl solution. The incorporation of PDA-MoS_2 shifted the polarization curves to lower current densities and higher corrosion potentials compared to the control sample, indicating enhanced corrosion resistance [27]. Figure 5b shows the EIS Nyquist plots of the asphalt samples. The semicircle's diameter in the Nyquist plot is a representation of the charge transfer resistance (Rct), which has an inverse relationship with the corrosion rate. The PDA-MoS_2 modified asphalt exhibited larger semicircle diameters compared to the control sample, indicating higher Rct values and improved corrosion resistance [28]. The improved ability of the PDA-MoS_2-asphalt to resist corrosion is due to the barrier created by the evenly distributed PDA-MoS_2 particles, preventing corrosive substances from penetrating the asphalt.

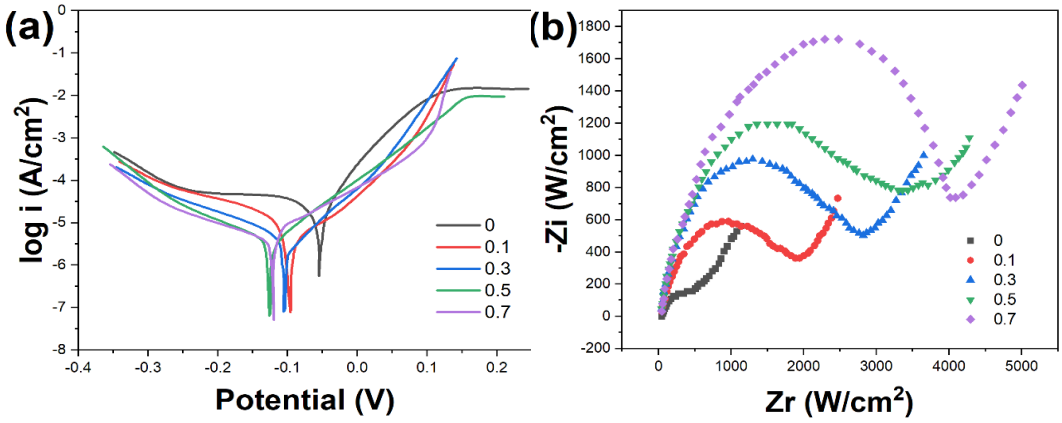

Fig. 5. (a) Potentiodynamic polarization curves and (b) EIS Nyquist plots of SBS-asphalt with different PDA-MoS_2 contents in 3.5 wt% NaCl solution.

3.3. Mechanisms for property enhancement

The addition of PDA-MoS_2 had a notable impact on the microstructure of the SBS-modified asphalt. As shown in Figure 6, the SEM images reveal the differences in the morphology of the asphalt samples. The control SBS modified asphalt (Figure 6a) exhibited a relatively smooth and homogeneous surface with some SBS polymer phases dispersed in the asphalt matrix. With the addition of PDA-MoS_2 (Figure 6b-d), the asphalt samples displayed a rougher surface morphology with well-dispersed PDA-MoS_2 particles. The PDA-MoS_2 particles were embedded in the asphalt matrix and formed a compact network structure, which contributed to the reinforcement of the asphalt [29]. The particle size of PDA-MoS_2 ranged from 1 to 3 μm, and no significant agglomeration was observed, indicating good dispersion stability. The improved microstructure of the PDA-MoS_2 modified asphalt can be attributed to the enhanced compatibility and interfacial adhesion between PDA-MoS_2 and the asphalt matrix, which results from the hydrophilic nature and functional groups of the PDA coating.

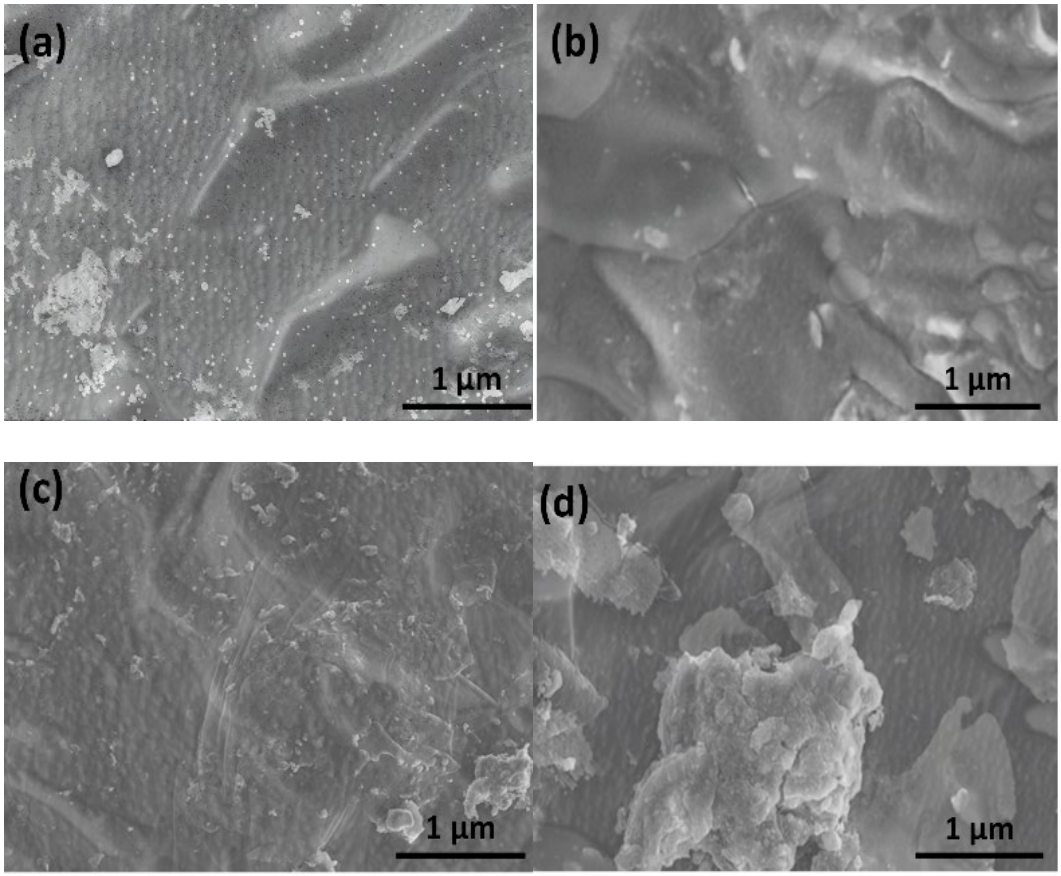

Fig. 6. SEM images of (a) control SBS-asphalt, and SBS-asphalt with (b) 0.1 wt%, (c) 0.3 wt%, and (d) 0.7 wt% PDA-MoS_2.

The chemical composition of the SBS-asphalt was altered by the incorporation of PDA-MoS_2, as evidenced by the FTIR spectra shown in Figure 7. The control SBS modified asphalt exhibited characteristic peaks of asphalt binder, such as the C-H stretching vibrations at 2920 cm^{-1} and 2850 cm^{-1}, and the C=C stretching vibration at 1600 cm^{-1} [30]. With the addition of PDA-MoS_2, new peaks emerged in the FTIR spectra. The peak observed at 3420 cm^{-1} was identified as the O-H stretching vibration of catechol hydroxyl groups in PDA. Additionally, the peaks at 1510 cm^{-1} and 1288 cm^{-1} were assigned to the C=C stretching vibration of aromatic rings and the C-O stretching vibration in PDA, respectively, as reported in previous studies [31]. The intensity of these peaks increased with increasing PDA-MoS_2 content, confirming the successful incorporation of PDA-MoS_2 into the asphalt matrix. The presence of PDA functional groups in the modified asphalt enhances the interfacial interactions and chemical bonding between PDA-MoS_2 and the asphalt components, leading to improved performance properties.

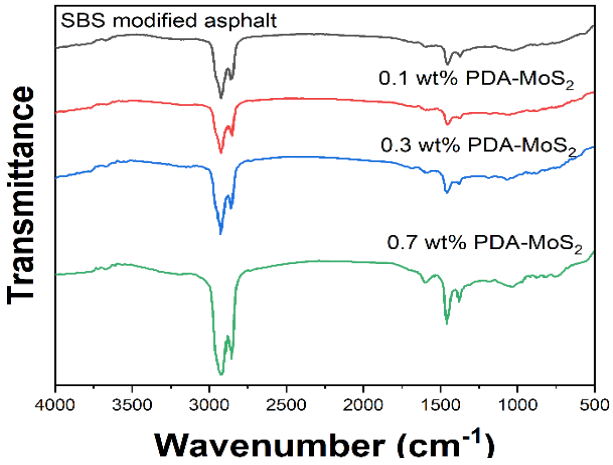

Fig. 7. FTIR spectra of SBS-asphalt with different PDA-MoS_2 contents.

The addition of PDA-MoS_2 greatly enhanced the water affinity of the SBS-asphalt mixture. The control SBS modified asphalt showed a water contact angle of 105.2 ± 1.5°, indicating a hydrophobic surface. With the addition of PDA-MoS_2, the water contact angle gradually decreased, reaching 68.1 ± 1.8° for the 0.7 wt% PDA-MoS_2 modified asphalt. The increased water affinity of the PDA-MoS_2 modified asphalt is due to the inclusion of hydrophilic functional groups like catechol hydroxyl and amine groups within the PDA layer [32]. The enhanced hydrophilicity facilitates the dispersion and compatibility of PDA-MoS_2 in the asphalt matrix, leading to better interfacial adhesion and improved performance properties. Moreover, the hydrophilic nature of PDA-MoS_2 can also enhance the moisture resistance of the modified asphalt by preventing the penetration of water into the asphalt matrix [33].

The improved performance characteristics of the PDA-MoS_2 enhanced asphalt can be credited to the combined impact of its components working together. The PDA coating on the surface of MoS_2 particles acts as a compatibilizer, improving the interfacial interactions and chemical bonding between MoS_2 and the asphalt matrix. The catechol and amine groups in PDA can form hydrogen bonds and π-π interactions with the polar functional groups in the asphalt, such as sulfoxide and carbonyl groups. These strong interfacial interactions enhance the adhesion and compatibility between PDA-MoS_2 and the asphalt matrix, leading to better dispersion and reinforcement effects. Moreover, the SBS polymer in the modified asphalt can also interact with the PDA-MoS_2 particles through physical entanglement and van der Waals forces, further enhancing the network structure and mechanical properties of the asphalt. The synergistic effect between PDA-MoS_2, SBS, and the asphalt matrix results in improved rheological properties, rutting resistance, and durability of the composite modified asphalt.

4. Conclusion

In conclusion, this study successfully developed a novel SBS composite modified asphalt incorporating PDA-MoS_2 with superior performance characteristics. The addition of PDA-MoS_2 significantly enhanced the properties of SBS-asphalt, with optimal results achieved at 0.7 wt% PDA-

MoS_2 content. Viscoelastic properties were markedly improved, with the rutting factor at 60°C increasing by 137% compared to the control sample. MSCR tests revealed enhanced rutting resistance, with Jnr values decreasing from 2.45 kPa^{-1} to 0.68 kPa^{-1} at 0.1 kPa stress level, and percent recovery increasing from 8.2% to 45.6%. Corrosion resistance was also significantly improved, as evidenced by electrochemical measurements. The mechanisms behind these enhancements were elucidated through microstructural and chemical analyses, revealing well-dispersed PDA-MoS_2 particles forming a compact network structure within the asphalt matrix. The synergistic effect between PDA-MoS_2, SBS, and asphalt components, facilitated by improved interfacial interactions and chemical bonding, resulted in the observed performance improvements. The hydrophilicity of the modified asphalt increased, with the water contact angle decreasing from 105.2° to 68.1°. These findings demonstrate the potential of PDA-MoS_2 as an effective modifier for SBS modified asphalt, offering a promising solution for enhancing the durability and performance of asphalt pavements under challenging conditions.

Acknowledgements

This work has been supported by Key Scientific and Technological Project of Henan Province (Grant No. 232102240024).

References

[1] Z. Hossain, B. Bairgi, M. Zaman, R. Bulut, in Geo-Chicago 2016 (American Society of Civil Engineers, 2016), pp. 477-487.

[2] C. Yan, W. Huang, P. Lin, Y. Zhang, Q. Lv, Fuel 252, 417 (2019); https://doi.org/10.1016/j.fuel.2019.04.022

[3] C. Yu, K. Hu, G. Chen, R. Chang, Y. Wang, Journal of Zhejiang University-SCIENCE A 22, 528 (2021); https://doi.org/10.1631/jzus.A2000359

[4] I. D. Uwanuakwa, M. Adamu, S. I. A. Ali, P. Akpinar, M. R. M. Hasan, K. A. Shariff, I. K. Umar, S. I. Haruna, Innovative Infrastructure Solutions 8, 89 (2023); https://doi.org/10.1007/s41062-023-01056-2

[5] X. Xie, K. Wang, M. Bao, G. Li, J. Shao, B. Du, Y. He, Journal of Molecular Modeling 29, 337 (2023); https://doi.org/10.1007/s00894-023-05746-7

[6] C. Li, G. Zeng, M. Zhou, Y. Fang, Z. Chen, Y. Xu, S. Ding, M. Yuan, H. Li, S. Wu, Materials Research Express 8, 035501 (2021); https://doi.org/10.1088/2053-1591/abe975

[7] K.-N. Kim, T. H. M. Le, Polymers 15, 2504 (2023); https://doi.org/10.3390/polym15112504

[8] X. Yao, C. Li, T. Xu, Construction and Building Materials 346, 128502 (2022); https://doi.org/10.1016/j.conbuildmat.2022.128502

[9] P. Wang, H.-R. Wei, X.-Y. Liu, R.-B. Ren, L.-Z. Wang, Sustainability 13, 10582 (2021);

https://doi.org/10.3390/su131910582

[10] L. Feng, P. Zhao, T. Chen, M. Jing, Polymers 14, 4121 (2022); https://doi.org/10.3390/polym14194121

[11] C. Shi, Y. Wu, T. Wang, Y. Yu, H. Wang, J. Yang, Materials and Structures 56, 33 (2023); https://doi.org/10.1617/s11527-023-02122-y

[12] I. Asi, Y. Khalayleh, International journal of pavement research and technology (2010).

[13] D. Han, G. Hu, and J. Zhang, Polymers 15, 256 (2023); https://doi.org/10.3390/polym15020256

[14] P. Leiva-Padilla, F. Moreno-Navarro, G. Iglesias, M. C. Rubio-Gamez, Infrastructures 5, 23 (2020); https://doi.org/10.3390/infrastructures5030023

[15] X. Zhu, Y. Wang, M. Miljković, R. Li, G. Hao, Construction and Building Materials 411, 134446 (2024); https://doi.org/10.1016/j.conbuildmat.2023.134446

[16]. S. Sun, T. Jiao, R. Xing, J. Li, J. Zhou, L. Zhang, Q. Peng, RSC Advances 8, 21644 (2018); https://doi.org/10.1039/C8RA02964D

[17] J. Gao, M. Zhang, J. Wang, G. Liu, H. Liu, Y. Jiang, ACS Omega 4, 4012 (2019); https://doi.org/10.1021/acsomega.9b00155

[18] H. Tian, X. Wu, K. Zhang, Membranes 11, 96 (2021); https://doi.org/10.3390/membranes11020096

[19] Q. Wang, F. Jia, S. Song, Y. Li, Separation and Purification Technology 236, 116298 (2020); https://doi.org/10.1016/j.seppur.2019.116298

[20] Q. Wang, L. Peng, Y. Gong, F. Jia, S. Song, Y. Li, Journal of Molecular Liquids 282, 598 (2019); https://doi.org/10.1016/j.molliq.2019.03.052

[21] Y. Sui, P. Li, X. Dai, C. Zhang, Reactive and Functional Polymers 165, 104965 (2021); https://doi.org/10.1016/j.reactfunctpolym.2021.104965

[22] P. Yan, M. Li, J. Liu, Y. Hu, K. Tang, Macromolecular Materials and Engineering 307, 2100654 (2022); https://doi.org/10.1002/mame.202100654

[23] Y. Wu, W. Ding, J. Li, Journal of Nanomaterials 2021, 6668393 (2021).

[24] A. H. Abed, H. U. Bahia, Construction and Building Materials 236, 117604 (2020); https://doi.org/10.1016/j.conbuildmat.2019.117604

[25] F. Moreno, M. Sol, J. Martín, M. Pérez, M. Rubio, Materials & Design 47, 274 (2013); https://doi.org/10.1016/j.matdes.2012.12.022

[26] Z. Liu, X. Liu, G. Zheng, K. Dai, C. Liu, C. Shen, R. Yin, Z. Guo, Polymer Testing 58, 227 (2017); https://doi.org/10.1016/j.polymertesting.2017.01.002

[27] C. Chen, G. Li, J. Zhu, Y. Lu, M. Jiang, Y. Hu, Z. Shen, X. Zhang, Carbon 120, 380 (2017); https://doi.org/10.1016/j.carbon.2017.05.072

[28] R. Swaminathan, P. Pazhamalai, V. Mohan, K. Krishnamoorthy, S.-J. Kim, Journal of Colloid and Interface Science 652, 845 (2023); https://doi.org/10.1016/j.jcis.2023.07.143

[29] N. S. A. Yaro, M. B. Napiah, M. H. Sutanto, A. Usman, S. M. Saeed, Case

Studies in Construction Materials 15, e00783 (2021); https://doi.org/10.1016/j.cscm.2021.e00783

[30] S. Luo, J. Tian, Z. Liu, Q. Lu, K. Zhong, X. Yang, Measurement 151, 107204 (2020); https://doi.org/10.1016/j.measurement.2019.107204

[31] Z. Feng, F. Cai, D. Yao, X. Li, Construction and Building Materials 273, 121713 (2021); https://doi.org/10.1016/j.conbuildmat.2020.121713

[32] M. Chen, J. Geng, C. Xia, L. He, Z. Liu, Construction and Building Materials 294, 123610 (2021); https://doi.org/10.1016/j.conbuildmat.2021.123610

[33] Y. Gong, J. Xu, R. Chang, E. Yan, Construction and Building Materials 273, 121758 (2021); https://doi.org/10.1016/j.conbuildmat.2020.121758